README File

OMAERUV V1.8.9.1

Released Date: May 31 2017

1. Overview

The NASA OMI aerosol data products generated by the OMAERUV algorithm are aerosol extinction optical depth (AOD), aerosol absorption optical depth (AAOD), and single scattering albedo (SSA) at 354, 388 and 500 nm. In addition, the UV Aerosol Index (UVAI) is calculated from 354 and 388 nm radiances.

AOD is a dimensionless measure of the extinction of light by aerosols due to the combined effect of scattering and absorption, while AAOD is that only due to aerosol absorption. The AI is simply a residual parameter that quantifies the difference in spectral dependence between measured and calculated near UV radiances assuming a purely molecular atmosphere. Because most of the observed residuals are associated with the presence of absorbing aerosols, this parameter is commonly known as the UV Aerosol Index (UVAI).

The OMAERUV retrieval algorithm uses a set of aerosol models to account for the presence of carbonaceous aerosols from biomass burning (BIO), desert dust (DST), and sulfate-based (SLF) aerosols (see Appendix 1). The optical depth and single scattering albedo values at 388 nm are inverted from radiance observations. Conversions to 354 and 500 nm are carried out to facilitate comparisons with measurements from other space-borne and ground based sensors, as well as with model calculations, which often report values at 500 nm. Because this transformation relies on the spectral dependence of the aerosol models assumed in the algorithm, the reported values at the other wavelengths, particularly those at 500 nm, should be considered less reliable.

For environments where cloud free conditions prevail, AOD can be reliably retrieved. Cloud interference with the satellite retrieval is minimal over arid and semi-arid regions where dust aerosols are commonly present. Clear skies are also frequent in areas of seasonal biomass burning and forest fires in the vicinity of the sources. As the plumes of dust and smoke aerosols drift away from their source regions, they mix with clouds and the AOD retrieval becomes very challenging. Because of the large sensitivity of the OMI near UV observations to particle absorption, the AAOD is the most reliable quantitative OMAERUV aerosol parameter.

The UVAI has become an invaluable tool for tracking long-range transport of absorbing aerosols (smoke and dust) throughout the globe, even when the aerosols are over clouds. The UVAI has been instrumental in the discovery of

important aspects of aerosol transport both horizontally and vertically. For instance, UVAI observations indicate that smoke aerosol plumes generated by boreal forest fires at mid and high latitudes are associated with the formation of pyro-cumulonimbus clouds capable of transporting carbonaceous aerosols to the lower stratosphere.

Effective this release, the OMAERUV UVAI becomes the official NASA Aerosol Index product, replacing the OMTO3-generated product which will no longer be produced in the upcoming version of the OMTO3 algorithm. The NASA OMI UVAI product continues the long-term record initiated in 1978 by the TOMS sensors.

This document provides a brief description of the OMAERUV Level-2 aerosol data products derived from observations by the Ozone Monitoring Instrument (OMI) on the EOS-Aura satellite. In the global mode each file contains a single orbit of data covering the sunlit portion of the Earth from pole-to-pole with a swath width of approximately 2600 km. The Level-2 file also contains the geo-location information associated with the geographic center of each OMI pixel in the global observation mode as well as the geographical coordinates of the corners of each pixel. Ancillary information used in the inversion procedure is also included in the file.

The information in this README file applies only to the third public release of the OMAERUV data of collection 3. As subsequent data versions are produced and released, the README file will be updated accordingly to reflect the latest algorithm modifications and data quality assessments. The OMAERUV algorithm is one of two OMI algorithms that are used to characterize the atmospheric aerosol load.

. Please refer to the OMAERUV release specific information file for details on formats and field name of variables, as well as software versions. and known problems.

2. Algorithm Upgrades in Version V1.8.9.1

A brief listing of the algorithm upgrades implemented in the current release is presented here. A more detailed description of the upgrades is given in the Algorithm Description section below. For a history of algorithm upgrades see appendix 2.

- Introduced a dynamic approach developed for the OMTO3 product to detect and flag row-anomaly-affected data. This change implemented in version 1.4.2 but not documented in the readme file.

-Replaced the CERES/SARB surface type data (180 x 360) with the high resolution data of a 1/6 degree (1080x 2160) Available at

http://mynasadata.larc.nasa.gov/thredds/catalog/las/surface_cover/catalog.html?dataset=las/surface_cover/data_usr_local_fer_data_data_IGBPa_2006.1deg.nc.jnl

- Introduced a new way of calculating OMAERUV UVAI using Mie Theory to represent cloud effects. Details of the new UVAI definition are discussed in section 3.

-Additional pressure node (800 mb) was added to the look-up tables used for the AI calculation. Now radiances are simulated for three surface pressure levels (600, 800 and 1013mb).

-Revisited Aerosol model selection and retrieval approach (see Table 3).

-Retrieval results for retrieval quality flags other than 0 and1 are no longer reported.

-The minimal UVAI value for aerosol retrievals over the ocean was changed from 0.8 to 1.0.

-Modified the criteria for assigning retrieval quality flags (see Figure 2).

-Introduced a smoothing function to transition from Southern to Northern Hemisphere COI threshold values used for aerosol type selection. This modification eliminates the abrupt discontinuity in aerosol type near the Equator.

-Updated UV-VIS spectral dependence of carbonaceous and sulfate aerosols for conversion of retrievals from 388 to 500nm.

-Developed new surface albedo data based on in-house climatology of 10-year long OMI observation. See section 3 for a detailed discussion.

-Applied Fresnel Correction to ocean surface albedo data-base.

-Introduced a new dust aerosol model accounting for asphericity of desert dust particles.

-Eliminated single channel retrieval approach. See Section 3 for details.

-Geographical coordinates of pixel corners are reported in addition to the center of pixel geolocation.

- Introduced the *HeightFlags* and *AIRSCO_Flags* data fields to document the options available to determine the values of aerosol layer height and CO index (COI) to be used in the algorithm.

3. V1.8.9.1 Algorithm Description

Though OMI is a hyper-spectral instrument and measures over a wide wavelength range from UV to blue (270-500nm), the OMAERUV aerosol algorithm currently uses the measurements made at just two wavelengths: 354 and 388 nm. This is partly to maintain heritage with similar algorithm used for TOMS [*Torres et al,* 1998], and partly because of a lack of reliable surface reflectance data at the longer OMI wavelengths. Wavelengths below 330 nm cannot be used due to strong ozone absorption.

3.1 Ancillary Information

3.1.1 Surface Albedo

A global climatological data set of Lambertian surface reflectivity (R_{SFC}) *at 354 and 388 nm is used in OMAERUV. It was obtained using a multi-year record of scene reflectivity (R_{SCE}) obtained from OMI observations. For a Lambertian reflecting surface* the satellite measured radiance at the top of the atmosphere can be estimated using the Chandresekar approximation (equation 1),

$$I^{obs} = I^{0} + \frac{RT}{1 - S_b R} \quad (1)$$

where I^{obs} represents the satellite measured radiance and, I^{0}, T, and S_b are respectively the modeled path radiance, the two-way transmittance, and the spherical albedo of a molecular atmosphere, and R is simply the Lambertian reflectivity of the of bottom of the atmospheric column that in addition to the actual surface, also includes clouds and aerosol effects. Scene Lambert Equivalent Reflectivity (LER) values at 354 and 388 nm (R_{SCE}) are calculated at every OMI pixel for a purely molecular atmosphere model solving for the R term in equation (1) yielding

$$R_{SCE} = \frac{I^{obs} - I^{0}}{T + S_b (I^{obs} - I^{0})} \quad (2)$$

The multi-year long record of R_{SCE} record has been used to create a monthly climatology of surface reflectivity (R_{SFC}) using the approach described below.

Over land, R_{SFC} is estimated as the minimum observed R_{SCE} over 10-years (2005-2014) for every month of the year averaged over a 0.25°x0.25° geographical grid. This climatological data set differs from that of *Kleipool et al* [2008], used in OMI's trace gas retrieval algorithm, in that the resulting surface albedo is associated with the actual observed minimum value per grid per month and, therefore, more suitable for aerosol retrieval applications.

The ocean surface reflectivity is estimated in a similar way as over land with the addition of a correction for the Sun's specular reflection. The satellite derived R_{SCE} under cloud-free conditions over the ocean is approximated as the sum of two terms: a Lambert-equivalent Fresnel reflectivity (R_F) term and a second reflectivity term associated with water-leaving reflectance (R_W). The R_F term is obtained by calculating the upwelling radiance at the top of the atmosphere using an atmosphere-ocean radiative transfer model [*Cox and Munk*, 1954] for a chlorophyll-free ocean. The calculated radiance is then converted to LER using an equation similar to Eq. 1, in which the calculated radiance is used in lieu of the observed one. The R_F thus calculated varies with solar zenith, view zenith and azimuth angles. R_W is estimated empirically by subtracting R_F from R_{SCE}. The resulting minimum R_W values per grid per month are assumed here to represent the ocean $R_{SFC.}$

The OMI-based surface reflectivity climatology is available from the PI upon request. This data set replaces a climatological data set similarly derived from TOMS long-term record used in the previous version.

3.1.2 Aerosol Layer Height

The height above the surface of absorbing aerosol layers (desert dust and smoke particles) is given by a climatological data set derived from CALIOP observations [*Torres et al.,* 2013]. Although the climatology covers most regions of the globe where seasonally varying atmospheric loads of desert dust and carbonaceous aerosols are known to reside, there are cases where the CALIOP data base does not provide height information. In those instances, the height of DST aerosol layers is taken from a GOCART-generated climatology [*Ginoux et al.,* 2001]. A detailed description of aerosol layer height determination is given in section 3.2.2.

3.1.3 Real Time AIRS Carbon Monoxide (CO)

Since CO is the main gaseous component of biomass burning, it constitutes a reliable tracer of carbonaceous aerosol. The AIRS/Aqua L3 Daily Standard Physical Retrieval V006 CO product (AIRS3STD) is used in the aerosol algorithm to aid in the identification of carbonaceous aerosols. As used in OMAERUV, AIRS3STD CO total column in molecules-cm^{-2} is reduced to a unitless index (COI), by dividing the AIRS reported CO measurement by 10^{18} molecules-cm^{-2} [*Torres et al.,* 2013].

3.2 OMAERUV Aerosol Products

3.2.1 Absorbing UV Aerosol Index and Cloud Fraction

The UVAI is a measure of the departure of the spectral dependence of the near-UV upwelling radiation at the top of the actual Earth surface-atmosphere system from that of a hypothetical pure molecular atmosphere bounded at the bottom by a wavelength independent Lambertian surface. The UVAI calculated as shown in Eq. 3, was developed empirically from TOMS observations. In Eq. 2, λ_0 is the reference wavelength (388 nm) whereas λ is the wavelength at which AI is calculated (354 nm). Near-zero values of UVAI result when the radiative transfer processes accounted for in the simple Rayleigh scattering model adequately explain the observations. For a well-calibrated sensor, the non-zero residues are produced solely by geophysical effects, of which absorbing aerosols are by far the most important source of positive UVAI values. Non-absorbing aerosols yield small negative UVAI values but the difficulty to separate the non-absorbing aerosol signal from other non-aerosol related effects limits its usefulness.

$$UVAI = -100\left\{\log\left[\frac{I_{\lambda}^{obs}}{I_{\lambda_0}^{obs}}\right] - \log\left[\frac{I_{\lambda}^{cal}}{I_{\lambda_0}^{cal}}\right]\right\} = -100\log\left[\frac{I_{\lambda}^{obs}}{I_{\lambda}^{cal}}\right] \qquad (3)$$

A new approach of calculating the UVAI has been developed. The new method explicitly accounts for scattering effects of water clouds. It is based on analytical studies showing that the use of Mie scattering theory reproduces remarkably well the satellite observed field of backscattered UV radiation in a cloudy atmosphere [*Ahmad et al.,* 2004]. In this approach, it is assumed that the radiance measured by the sensor at pixel level emanates from a combination of clear and cloudy conditions (I_{λ}^{s} and I_{λ}^{C}) involving a cloud of fixed optical depth and varying cloud fraction. The I_{λ}^{s} term is calculated from the Chandrasekhar equation using as input the wavelength dependent climatological values of surface albedo (derived from analysis of the 10-year long-term OMI record of minimum reflectivity) and a pure molecular atmospheric model for surface pressured adjusted for topography. The I_{λ}^{C} terms, on the other hand, are calculated using Mie scattering theory for an assumed water cloud model [*Deirmendjian,* 1964] and wavelength-dependent refractive index [*Hale and Querry*, 1973], at prescribed top and bottom levels (700 and 800 hPa), and fixed cloud optical depth (COD). The choice of COD value of 10 is based on the highest frequency of occurrence of this value reported by MODIS observations [*King et al.,* 2013]. A wavelength independent radiative cloud fraction, f_C, is calculated from equation

$$f_C = \frac{I_{\lambda_0}^{obs} - I_{\lambda_0}^{s}}{I_{\lambda_0}^{C} - I_{\lambda_0}^{s}} \quad (4).$$

When the resulting cloud fraction is larger than unity, overcast sky conditions are assumed (i.e., f_C=*1.0*), and a new I_{λ}^{C} term for COD value larger than 10 that

matches $I_{\lambda_0}^{obs}$ is derived. I_{λ}^{cal} values are then obtained by linearly combining the clear and cloudy sky contributions:

$$I_{\lambda}^{cal} = (1.0 - f_C) I_{\lambda}^{s} + f_C I_{\lambda}^{C} \quad (5),$$

This way of calculating the I_{λ}^{cal} term is conceptually similar to the MLER method [*McPeters et al, 2007; Penning De Vries and Wagner*, 2011] used in the OMTO3 AI definition. The major difference is that while in the MLER approach clouds are modeled as Lambertian opaque surfaces using Rayleigh scattering calculations, the new method treats clouds as polydispersion of liquid water droplets, and uses Mie radiative transfer theory in the forward calculations.

The LER approach used in the previous OMAERUV version will still be used under conditions of snow/ice presence at the surface as indicated by the surface quality flag available in the level1b files. The LER approximation is also applied for high terrain regions with surface pressure lower than 600 hPa.

The Mie-Theory-based UVAI reduces significantly negative residual values associated with water clouds in the LER definition. In the new approach, the background UVAI is closer to zero, and, overall, the resulting values are higher by about 0.4 than those resulting from the previous model.

3.2.2 Aerosol Optical Depth and Single Scattering Albedo

In the UV, the reflectance of all terrestrial surfaces is very low compared to the atmospheric signal, therefore, the retrieval of aerosol optical depth is possible over both water and land surfaces, including the arid and semi-arid regions of the world that appear very bright in the visible and near-IR. In addition, the interaction between aerosol absorption and molecular scattering from below the aerosol layer allows the retrieval of aerosol single scattering albedo.

The current characterization of ocean reflective properties in the OMAERUV algorithm does not explicitly account for ocean color effects and, therefore, the quality of the retrieved aerosol properties over the oceans for low aerosol amounts would be highly uncertain. For that reason, retrievals over the oceans are only carried out for high concentrations of either desert dust or carbonaceous aerosols as indicated by UVAI values larger than or equal to 1.0. Over the oceans UVAI values less than 1.0 are assumed to be associated with ocean color effects and/or low concentration weakly absorbing (or non-absorbing) aerosols.

- Aerosol Models

The OMAERUV retrieval algorithm assumes that the column atmospheric aerosol load can be represented by one of three types of aerosols: desert dust (DST), carbonaceous aerosols associated with biomass burning (CRB), and sulfate-based aerosols (SLF). Each aerosol type is represented by seven aerosol

models of varying single scattering albedo, for a total of twenty-one models. The micro-physical properties of the twenty-one aerosol models used by OMAERUV are based on long-term statistics of ground-based observations by the Aerosol Robotic Network (AERONET). The CRB and SLF aerosol types are modelled as polydispersions of spherical particles. New with respect to this version are the DST models now modelled as spheroids (Torres et al., 2017; Gassó and Torres, 2016). For a full description of the aerosol models see Appendix 1. Radiance look-up tables at 354 and 388 nm with nodal points on viewing geometry, AOD, SSA and aerosol layer height are created using Mie Theory for spherical particles and T-matrix and Geometric Optics for spheroids [Dubovik et al., 2006].

- Aerosol type selection

Aerosol type determination is carried out on the basis of the magnitudes of the UVAI and COI parameters as illustrated in Fig. 1. Because of the lack of AIRS daily coverage, it is not always possible to use same-day COI values to infer aerosol type. Depending on AIRS data availability, COI may be determined based on current-day observations, previous day observations, or a monthly climatology. The actual source of COI data is documented in the *AIRSCO_Flags* data field with values from 1 to 3 as shown in Table 1.

Value of *AIRSCO_Flags* data field	**Source of COI data**
1	Current day
2	Previous day
3	Monthly Climatology

Table 1. COI determination

Threshold values of UVAI (*$UVAI_0$)* are 0.8 over land, and 1.0 over the oceans. COI threshold values (*COI_0*) are 2.0 and 1.6 for the northern and southern hemisphere respectively. *COI_0* values are intended to remove background upper tropospheric CO which may not be necessarily associated with carbonaceous aerosols. A smoothing function in *COI_0* is used to transition from SH to NH threshold values.

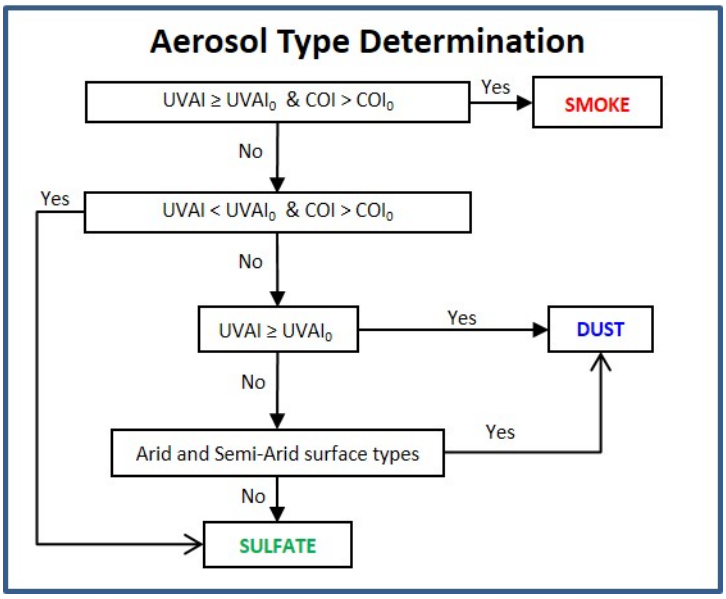

Figure 1. Flow diagram illustrating the aerosol type selection scheme.

-Cloud Screening

Sub-pixel cloud contamination is the largest source of uncertainty in retrieved quantitative OMI aerosol products. In OMAERUV the level of cloud contamination is determined in a decision tree using a combination of thresholds in reflectivity, R_{SFC} and ΔR (R_{SCE} - R_{SFC}), COI and UVAI as shown in Fig. 2. Algorithm quality flags 0 and 1 assign a level of confidence to the retrieved parameters. Flag 0 (highest confidence) is assigned to retrieval conditions when minimum cloud contamination is detected, whereas Flag 1 is reported for conditions where cloud contamination is suspected.

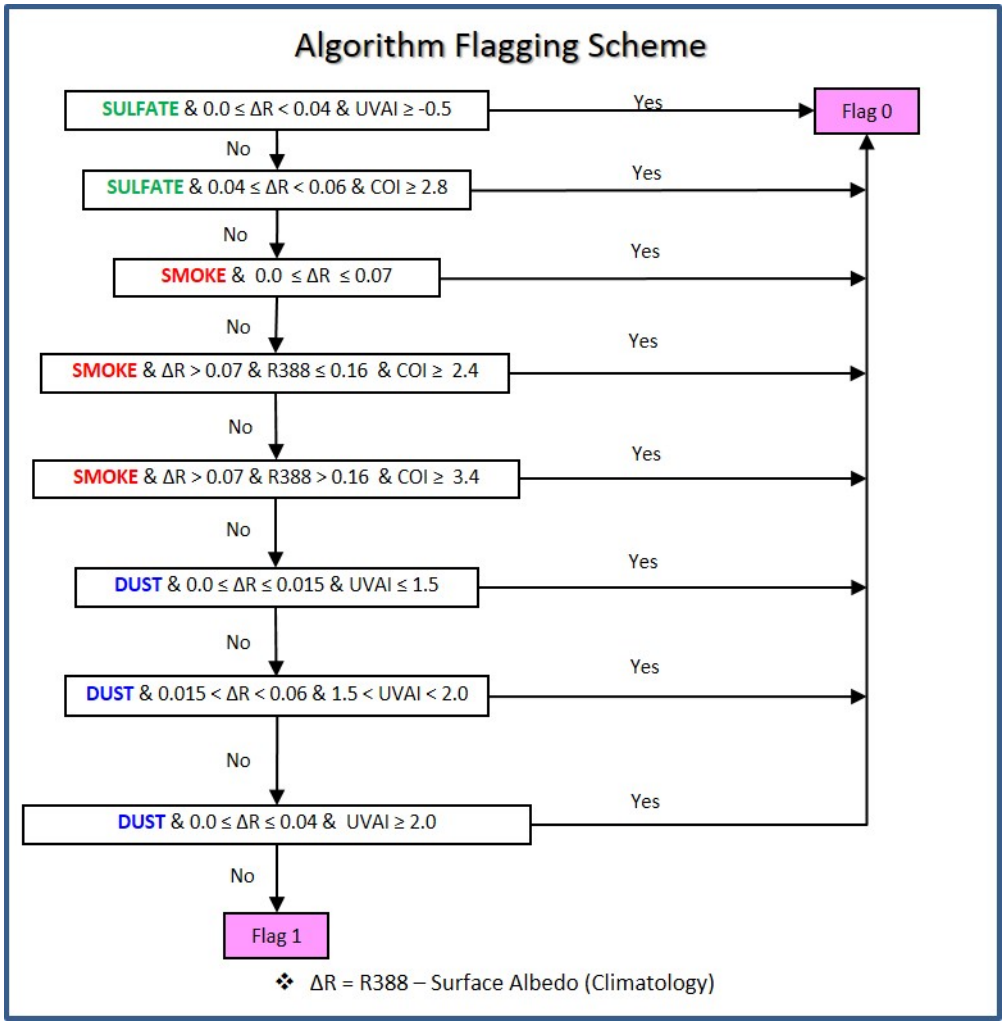

Figure 2. Criteria for identifying cloud-free pixels

Although, the data is still reported for flag 1 retrievals, its quantitative use is not recommended. Because cloud contamination affects AOD and single scattering co-albedo (1-SSA) in opposite directions, a partial cancellation of errors may take place in the calculation of AAOD.

- Aerosol layer height

The assumed aerosol level height is extracted from the CALIOP height climatology for each pixel as discussed in section 3.1.2. Although the CALIOP climatology provides information on aerosol layer height for most of the globe, there may be instances when no data is available. In those cases, the choice of aerosol layer height for absorbing aerosol layers varies with aerosol type and location.

Carbonaceous aerosol layers within 30 degrees of the Equator are assumed to have maximum concentration at 3 km above ground level; whereas

smoke layers at mid and high-latitude (poleward of ±45˚) are assumed to peak at 6 km. The height of smoke layers between 30˚ and 45˚ latitude in both hemispheres is interpolated between 3 and 6 km with latitude.

The height of desert dust aerosol layers varies between 1.5 and 10 km, and is taken from a multi-year climatological average of Chemical Model Transport (CTM) calculations using the GOCART model.

For the sulfate-based aerosols, the algorithm considers that the aerosol concentration is largest at the surface and decreases exponentially with height.

The *HeightFlags* data field provides information on the source of aerosol layer height used in the AOD/SSA retrieval. Value of *HeightFlags* varies from 1 to 4 as shown in Table 2.

Value of *HeightFlags* data field	Source of aerosol layer Height information
1	CALIOP Climatology
2	GOCART Climatology
3	Interpolated with latitude between 3 and 6 km
4	Assumed value (0.0, 1.5, 3.0, 6.0, or 10.0)

Table 2. Aerosol layer height determination

3.2.5 Retrieval Products

A summary of the retrieval criteria and retrieved parameters is presented in Table 3. As stated, retrievals take place over land for all cloud-free conditions. In addition of cloud-free conditions, the AI must be greater than unity for ocean retrievals.

Surface Category	*UVAI*	COI	Surface Type	Aerosol Type	Retrieved Parameters
Ocean	≥ 1.0	>2.0 NH (1.6 SH)	n/a	CRB	AOD, SSA
Ocean	≥ 1.0	≤2.0 NH (1.6 SH)	n/a	DST	AOD,SSA
Ocean	<1.0	-	-	-	No retrieval
Land	≥ 0.8	>2.0 NH (1.6 SH)	All	CRB	AOD,SSA
Land	≥ 0.8	≤ 2.0 NH (1.6 SH)	All	DST	AOD,SSA
Land	< 0.8	>2.0 NH (1.6 SH)	All	SLF	AOD,SSA
Land	< 0.8	≤ 2.0 NH (1.6 SH)	All but arid	SLF	AOD,SSA
Land	< 0.8	≤ 2.0 NH (1.6 SH)	arid	DST	AOD,SSA

Table 3. Retrieval Approach Criteria

Retrieved values of AOD, AAOD and SSA are reported at 388 nm. Similar values are also reported at 354 and 500 nm by conversion from the 388 nm retrieval. The wavelength conversion from 388 nm to 354 and 500 nm is done using the spectral dependence associated with the assumed aerosol particle size distribution and retrieved absorption information. The wavelength transformation for carbonaceous aerosols has been revisited to account for the presence of organic carbon.

3.2.6 Algorithm Flag

A simplified algorithm flag scheme has been implemented. Flag categories and their description are summarized in Table 4.

Flag	Description
0	Minimum sub-pixel cloud contamination. Most reliable retrievals(AOD, SSA, AAOD)
1	Possible Cloud contaminated retrievals, retrievals still reported.
2	No longer used.
3	Out-of-bounds SSA or AOD above 6.0 at 500nm.
4	Snow/ice contaminated data.
5	Solar Zenith Angle above threshold (70 degree).
6	Sun glint angle below threshold over water (40 degree).
7	Terrain Pressure below threshold (250.0 hPa).
8	Cross track anomaly.

Table4. Algorithm flag scheme

Flags 0 and 1 qualify the reliability of reported retrieved parameters in terms of sub-pixel cloud contamination effects. Flag 1 is reported for conditions where cloud contamination was suspected to be present. Although, the data is still reported for flag 1 retrievals, its quantitative use is not recommended.

Flags 3 thru 7 document the occurrence of observational, geographical or environmental conditions preventing the retrieval of aerosol parameters and fill values for the retrieved parameters are reported in the respective pixel.

Flag 8 is used to identify pixels affected by a condition known as the cross track or 'row' anomaly. It consists on an external blockage affecting the quality of the level 1B radiance data at all wavelengths for a number of OMI viewing directions. The affected viewing positions correspond to rows on the CCD detectors, and hence the term 'Row Anomaly' is used to refer to this instrumental issue. The OMI row anomaly is dynamic; it changes over time, and affects the quality of OMI Level 2 data products. By means of radiances analysis, row anomalies are identified and flagged by KNMI in the XTrackQualityFlags field of the OMI L1b data.

Starting with algorithm version 1.4.2, a row anomaly flagging scheme developed for the NASA OMI Total Ozone (OMTO3) product has been adopted in OMAERUV. In the OMTO3-based approach anomaly affected rows are identified determined through analysis of averages for each row of previous ten days of data. Upon reprocessing, the flags for each ten day period are determined using data from the same period. In OMAERUV row anomaly affected pixels are assigned Algorithm Flag 8 as shown in Table 2 and fill values are reported in the respective pixel.

More detailed description of the algorithm is available in the Algorithm Theoretical Basis Document (ATBD) on
http://eospso.gsfc.nasa.gov/eos_homepage/for_scientists/atbd/docs/OMI/ATBD-OMI-03.pdf

4. Data Quality Assessment

Because of the relatively large footprint of the OMI observations (13x24 km^2 at nadir), the major factor affecting the quality of aerosol products is sub-pixel cloud contamination. Currently the cloud mask is based on simple reflectivity, *UVAI* and COI thresholds (Figure 2), which can still allow significant overestimation of the mean AOD. However, experience with TOMS suggests that monthly mean AODs do reliably capture variation in the AOD with time. It is important to note, however, that the AAOD is less affected by cloud contamination and hence is more reliable.

In general OMAERUV retrievals are more reliable over land than over water surfaces. The near-UV retrieval method is particularly sensitive to carbonaceous and mineral aerosols. The sources of these aerosol types are located over the continents, and the atmospheric aerosol load associated with these events is generally large. In addition, dust and smoke aerosol events tend to take place under meteorological conditions which do not favor the formation of clouds in the vicinity of the sources, such as arid and semi-arid areas in the case of dust, and the dry season in the case of biomass burning. The OMAERUV retrieved AOD of sulfate-based aerosols is less accurate due to its low values, higher spatial variability and increased levels of sub-pixel cloud contamination.

Ocean OMAERUV retrievals are affected by other factors. In addition to sub-pixel clouds, the ocean surface reflectance show distinct angular and spectral variations (compared to land) due to spectrally varying scattering from the water, often called water-leaving radiances. (WLR), chlorophyll, sediments and other types of suspended matter decrease WLR. Spectral variations of ocean reflectance are accounted for making use of a climatology of wavelength dependent surface reflectance data set. Short-term variability, however, is not taken into account in the current version of the algorithm. Ocean retrievals of AOD and AAOD are not reported for sun glint angles smaller than 40º or for scenes where UVAI is less than1.0.

The AOD over land is expected to have the same root –mean square (rms) error as TOMS retrievals (0.1 or 30% whichever is larger). The rms error in AOD over water is likely to be 2 times larger. The rms error for AAOD is estimated to be ~0.01.

Density plot comparisons of OMAERUV retrieved optical depth to AERONET observations at 44 sites [Ahn et al., 2014] for current (left) and previous (right) OMAERUV versions are shown in Figure 3. The sample comparison includes sites the three aerosol types considered in the algorithm are present. An important increase in correlation coefficient is evident. Only minor changes in slope and y-intercept are observed. The percent of points retrievals within the lasgest og 0.1 or 30% (Q) in the new version is comparable to that in the previous one.

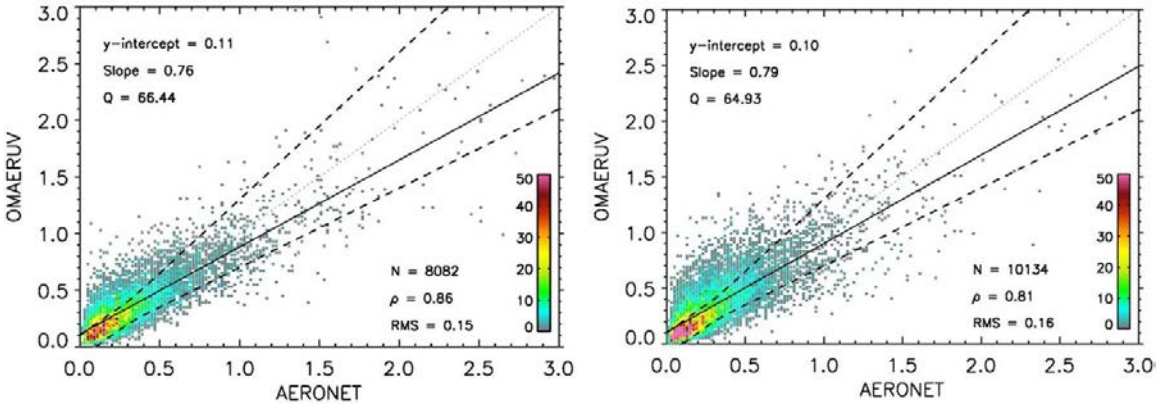

Figure 3. OMAERUV-AERONET comparison of aerosol optical depth, for current (left) and previous algorithm versions.

For environments where sub-pixel cloud contamination is persistent during all seasons the statistics of the OMAERUV-AERONET comparisons are poor. For these conditions comparisons over a longer period are needed to better assess the quality of the OMI aerosol product.

As part of the data quality assessment OMAERUV retrievals of AOD have been compared to MODIS data for different aerosol types. In general, when clear conditions predominate, the OMAERUV and MODIS AOD products are well correlated, especially for large-scale dust and smoke events. For background aerosol conditions, sub-pixel cloud contamination significantly affects the OMI retrieval.

The OMAERUV retrieved 388 nm single scattering albedo has been evaluated by comparison to AERONET retrievals at several sites [Jethva et al., 2014]. Figure 4 shows AERONET – OMAERUV SSA comparisons for current (left) and previous (right) versions of the OMI algorithm. Comparisons were done using all available AERONET retrievals for the period 2004-20013. Because of the lack of AERONET near UV observations, the OMI results have been converted to 440 nm to facilitate this analysis. Overall, a higher percentage of current version OMAERUV SSA retrievals agree with AERONET results within 0.03 (dashed lines) and 0.05 (dotted lines) relative to the previous version.

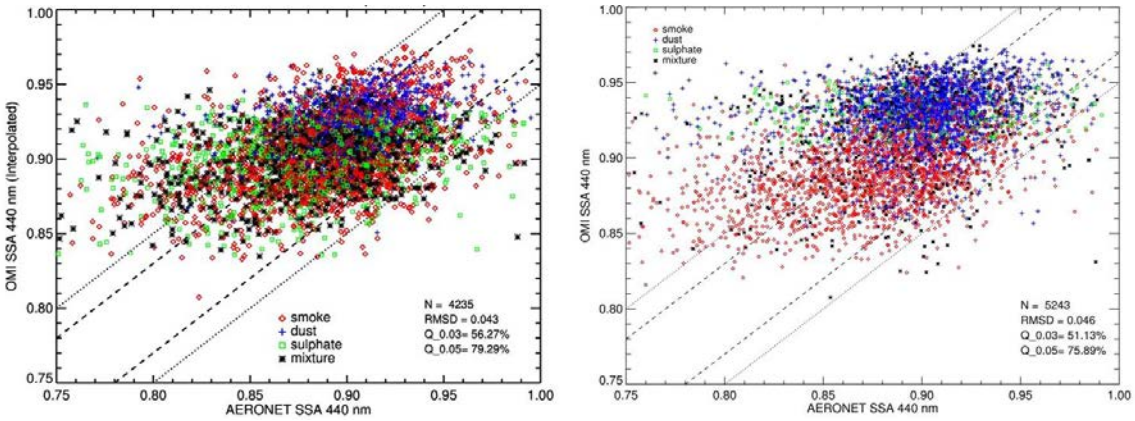

Figure 4. OMAERUV-AERONET comparison of single scattering albedo for current (left) and previous versions of the algorithm.

5. Product Description

A 2600-km wide OMI swath contains 60 pixels. Due to optical aberrations and a small asymmetry between the instrument optic axis with the spacecraft nadir, the pixels on the swath are not symmetrically aligned on the line perpendicular to the orbital plane. The reported center-of-pixel latitude and longitude represent the location of each pixel on the ground to a fraction of a pixel. Geographical coordinates of the four corners of each pixel are also provided.

The OMAERUV product is written as an HDF-EOS5 swath file. For tools to read HDF-EOS5 data files, please visit the link: http://disc.gsfc.nasa.gov/Aura/tools.shtml.

A single OMAERUV file contains information retrieved from each OMI pixel over the sun-lit portion of one Aura orbit. The data are ordered in time.

These files includes latitude, longitude, viewing geometry, best estimate values of AOD (variable name FinalAerosolOpticalDepth) and AAOD (variable name FinalAerosolAbsOpticalDepth) at 352, 388 and 500 nm associated with a reported particular choice of aerosol vertical distribution, and ancillary parameters used in the retrieval scheme as well as diagnostic flags.

A very important parameter also reported is the algorithm quality flag (field name FinalAlgorithmFlags), which contains integer values indicating a confidence level in cloud screening. Most users should use data with quality flag 0 and 1 depending on their applications. For a complete list of the parameters, please read the OMAERUV file specification. Gridded products are also available. Please check the Goddard Earth Sciences (GES) Data and Information Services Center (DISC) website for current information on these products.

OMAERUV aerosol data, over many ground stations and along Aura validation aircraft flights paths are also available through the Aura Validation Data Center (AVDC) website to those investigators who are associated with the various Aura science teams.

Questions related to the OMAERUV aerosol dataset should be directed to the GES DISC. For questions and comments related to the OMAERUV aerosol algorithm and data quality, please contact Omar Torres (omar.o.torres@nasa.gov) who has the overall responsibility for these products.

References and related publications

Ahmad, Z., P. K. Bhartia, and N. Krotkov (2004), Spectral properties of backscattered UV radiation in cloudy atmospheres, J. Geophys. Res., 109, D01201, doi:10.1029/2003JD003395.

Ahn, C., O. Torres, and H. Jethva (2014), Assessment of OMI near-UV aerosol optical depth over land, J. Geophys. Res. Atmos., 119, 2457–2473, doi:10.1002/2013JD020188.

Ahn C., O. Torres, and P.K. Bhartia (2008), Comparison of OMI UV Aerosol Products with Aqua-MODIS and MISR observations in 2006, *J. Geophys. Res*, 113, D16S27, doi:10.1029/2007JD008832.

Cox, C., and W. Munk (1954) Measurement of the roughness of the sea surface from photographs of the Sun's glitter, J. Opt. Soc. Amer., 44, 838–850.

Dave, J.V., and C.L. Mateer (1967), A preliminary study on the possibility of estimating total atmospheric ozone from satellite measurements, *J. Atm Sci.,* 24, 414-427

Deirmendjian, D (1964), Scattering and polarization properties of water clouds and hazes in the visible and infrared, Appl. Opt., 3, 187–196.

Dubovik, O., *et al. (*2006*),* Application of spheroid models to account for aerosol particle nonsphericity in remote sensing of desert dust, *J. Geophys. Res.*, 111, *D11208, doi:*10.1029/2005JD006619.

Fromm, M., R. Bevilacqua, R. Servranckx, J. Rosen, J.P. Thayer, J. Herman, and D. Larko, Pyro-cumulonimbus injection of smoke to the stratosphere: Observations and impact of a super blowup in northwestern Canada on 3-4 August 1998, J. Geophys. Res.,110, doi:10.1029/2004JD005350, 2005

Gassó, S. and Torres, O.: The role of cloud contamination, aerosol layer height and aerosol model in the assessment of the OMI near-UV retrievals over the ocean, Atmos. Meas. Tech., 9, 3031-3052, doi:10.5194/amt-9-3031-2016, 2016

Ginoux, P., M. Chin, I. Tegen, J. Prospero, B. Holben, D. Dubovik,and S. J. Lin, 2001: Sources and distributions of dust aerosols simulated with the GOCART model. *J. Geophys. Res.,* **106,** 20,255–20,273.

Herman, J.R., and E. A. Celarier, Earth surface reflectivity climatology at 340 and 380 nm from TOMS data, J. Geophys. Res., 102, 28,003-28,011, 1997

IGBP, http://www-surf.larc.nasa.gov/surf/pages/sce_type.html

Jethva, H., O. Torres, and C. Ahn (2014), Global assessment of OMI aerosol single-scattering albedo using ground-based AERONET inversion, J. Geophys. Res. Atmos., 119, doi:10.1002/2014JD021672.

Jethva, H. and O. Torres (2011): Satellite-based evidence of wavelength-dependent aerosol absorption in biomass burning smoke inferred from ozone monitoring instrument, Atmos. Chem. Phys. , 11, 10541-10551, doi:10.5194/acpd-11-7291-2011.

Joiner J. and A.P. Vasilkov, First Results From the OMI Rotational Raman Scattering Cloud Pressure Algorithm, IEEE Trans. Geo. Rem. Sens., 2006, Vol. **44**, No. 5, 1272-1282, doi:10.1109/TGRS.2005.861385.

Kleipool, Q. L., M. R. Dobber, J. F. de Haan, and P. F. Levelt (2008), Earth surface reflectance climatology from 3 years of OMI data, J. Geophys. Res., 113, D18308, doi:10.1029/2008JD010290.

Livingston,J.M, J. Redemann, P. B. Russell, O. Torres, B. Veihelmann, P. Veefkind, R. Braak, A. Smirnov, L. Remer, R. W. Bergstrom, O. Coddington, K. S. Schmidt, P. Pilewskie, R. Johnson, and Q. Zhang (2009), Comparison of aerosol optical depths from the Ozone Monitoring Instrument (OMI) on Aura with results from airborne sunphotometry, other space and ground measurements, Atmos. Chem. Phys. Discuss., 9, 6743-6765

McPeters, R. D., Bhartia, P. K., Krueger, A. J., Herman, J. R., Wellemeyer, C. G., Seftor, C. J., Jaross, G., Torres, O., Moy, L., Labow, G., Byerly, W., Taylor, S. L., Swissler, T., and Cebula, R. P (1998, Earth Probe Total Ozone Mapping Spectrometer (TOMS) Data Products User's Guide, NASA Technical Publication 1998-206895

Penning de Vries, M. and Wagner, T.: Modelled and measured effects of clouds on UV Aerosol Indices on a local, regional, and global scale, Atmos. Chem. Phys., 11, 12715-12735, doi:10.5194/acp-11-12715-2011, 2011.

Torres et al., (2017), Impact of the Ozone Monitoring Instrument Row Anomaly on the Long-term Record of Aerosol Products, *in preparation*

Torres, O., Ahn, C., and Chen, Z.: Improvements to the OMI near UV aerosol algorithm using A-train CALIOP and AIRS observations, Atmos. Meas. Tech., 6, 5621-5652, doi:10.5194/amtd-6-5621-2013, 2013.

Torres, O., A. Tanskanen, B. Veihelman, C. Ahn, R. Braak, P. K. Bhartia, P. Veefkind, and P. Levelt (2007), Aerosols and Surface UV Products from OMI Observations: An Overview, , *J. Geophys. Res.,* 112, D24S47, doi:10.1029/2007JD008809.

Torres O., P.K. Bhartia, J.R. Herman and Z. Ahmad, Derivation of aerosol properties from satellite measurements of backscattered ultraviolet radiation. Theoretical Basis, J. Geophys. Res., 103, 17099-17110, 1998

Torres, O., P.K. Bhartia, A. Syniuk, and E. Welton, TOMS Measurements of Aerosol Absorption from Space: Comparison to SAFARI 2000 Ground based Observations, J. Geophys. Res., 110, D10S18, doi:10.10129/2004JD004611, 2005

APPENDIX 1

OMI CRB AEROSOL MODELS

Real refractive index 1.50 (wavelength independent)

Models 1:4

R_F	R_C	σ_F	σ_C	Fraction
0.08	0.705	1.492	2.075	$2.05\ 10^{-4}$

Nodal points on imaginary refractive index (wavelength dependent):
354.0 nm: 0.0576, 0.0480, 0.0360, 0.0240
388.0 nm: 0.0480, 0.0400, 0.0300, 0.0200

Models 5:7

R_F	R_C	σ_F	σ_C	Fraction
0.087	0.567	1.537	2.203	$2.06\ 10^{-4}$

Nodal points on imaginary refractive index (wavelength dependent):
354.0 nm: 0.01200, 0.0060, 0.00000
388.0 nm: 0.01000, 0.0050, 0.00000

OMI SLF AEROSOL MODELS

Models 1:7

Real refractive index 1.40 (wavelength independent)

R_F	R_C	σ_F	σ_C	Fraction
0.088	0.509	1.499	2.160	$4.04\ 10^{-4}$

Nodal points on imaginary refractive index (wavelength dependent):
354.0 nm: 0.03600, 0.03000, 0.02400, 0.01800, 0.01200, 0.00600, 0.00000
388.0 nm: 0.03000, 0.02500, 0.02000, 0.01500, 0.01000, 0.00500, 0.00000

OMI DST AEROSOL MODELS

Real refractive index 1.55 (wavelength independent)

Models 1:7

R_F	R_C	σ_F	σ_C	Fraction
0.052	0.67	1.697	1.806	$4.35\ 10^{-3}$

Nodal points on imaginary refractive index (wavelength dependent):
354.0 nm: 0.02303, 0.01279, 0.00832, 0.00561, 0.00256, 0.00128, 0.00000
388.0 nm: 0.01662, 0.00923, 0.00600, 0.00405, 0.00185, 0.00092, 0.00000

The table below describes the distribution of spheroid axis ratio and associated weights assumed in the calculation of DST models phase function. Note that the fraction weights sum up to 1.00.

Axis Ratio	Fractional Weight
0.33490	0.0661850
0.36690	0.0650250
0.40190	0.0636350
0.44030	0.0620500
0.48230	0.0587200
0.52830	0.0533500
0.57870	0.0477625
0.63390	0.0429530
0.69440	0.0403205
0.76070	0.0000000
0.83330	0.0000000
0.91290	0.0000000
1.00000	0.0000000
1.09540	0.0000000
1.20000	0.0000000
1.31450	0.0000000
1.44000	0.0403205
1.57740	0.0429530
1.72800	0.0477625
1.89290	0.0533500
2.07360	0.0587200
2.27150	0.0620500
2.48832	0.0636350
2.72580	0.0650250
2.98600	0.0661850

R_F & R_c are radii for fine and coarse mode aerosols
$\sigma_{F\,\&}$ σ_C are the standard deviations

APPENDIX 2

History of Algorithm Upgrades

1. Algorithm Version V1.1.1 (October 31, 2007)

The use of a new calibrated OMI level1b (L1b) radiance data set is most important change in this release. The collection 003 L1b data includes a radiometric correction as well as an adjustment for stray light effects. The first correction is largely spectrally independent whereas the latter is wavelength dependent. The OMI L1b products are available through the NASA S4PA system (http://disc.gsfc.nasa.gov/Aura/OMI/index.shtml).

Threshold values of reflectivity and UV aerosol index used for aerosol type selection and assignment of algorithm flags were modified as shown in Table 1.

Sun glint angle threshold over the oceans for Aerosol Index calculation has been lowered from 40º to 20º.

2. Algorithm Version V1.1.6 (March 31, 2009)

A major algorithm modification was implemented earlier in this version. Aerosol retrievals over the oceans are carried out only if the AI is larger than one. When AI ≤ 1.0 no retrieval is performed and fill values are reported.

Over the oceans AI values less than one are associated with ocean color and/or low aerosol concentration weakly absorbing (or non-absorbing) aerosols. Since the current representation of ocean surface effects in the OMAERUV algorithm does not explicitly correct for ocean color signal, the quality of the retrieved aerosol properties over the oceans for low aerosol amounts is highly uncertain.

Other algorithm changes:

- Changes to aerosol retrieval over land for AI ≤1.0 (See algorithm description)

- Reported Retrieved Products: Aerosol Extinction Optical Depth, Aerosol Absorption Optical Depth and Single Scattering Albedo at 354, 388 and 500 nm.

- Changes in prescribed aerosol layer height when aerosol type is identified as carbonaceous (BIO). See Algorithm Description section below.

- Row anomaly Exclusions:

Several row anomalies have occurred in the recent past. These anomalies affect the quality of the OMAERUV data products. In this version of the Algorithm the following rows are excluded, i.e., no retrieval are reported

- Row Anomaly Exclusion Rules

1. (54 and 55; 1-based) since June 1, 2007.
2. (38 – 43) since May 1, 2008.
3. (36 – 45) since Dec 1, 2008
4. (29 – 45) since Jan 24, 2009.

Algorithm version 1.3.7 (October 20, 2011)

The carbonaceous (BIO) aerosol model has been replaced with a new model that includes wavelength-dependent imaginary component of the refractive index (see Appendix 1). This change allows for the presence of organic carbon (OC) as a light-absorbing aerosol component [Jethva and Torres, 2011]. The previous aerosol model implicitly assumed black carbon (BC) as the only absorbing component.

The differentiation between carbonaceous and desert dust aerosols has been improved by making use of column carbon monoxide (CO) measured by the AIRS sensor on the Aqua satellite. CO is the most abundant gaseous component of carbonaceous aerosols and is, therefore, a reliable tracer of biomass burning aerosols. The aerosol type selection is based on the combined use of the OMI UV Aerosol Index (AI) and the CO amount. The short time difference of only few minutes between Aura-OMI and Aqua-AIRS observations allows the use of the two observations to characterize almost the same scene. See section 3 for a detailed description of the procedure to identify the aerosol type.

A CALIOP-based climatology of aerosol layer height has been created. When either the BIO or DST aerosol type has been selected the aerosol layer height is primarily determined by a monthly global climatology derived from CALIOP observations. When the aerosol layer height is not available from CALIOP climatology (generally at high latitudes in both hemispheres) the height is still obtained, as in the previous version of the algorithm, based on the climatology from GOCART model inferred aerosol heights. See section 3 for details.

Changes in look-up table configuration have taken place. The number of solar zenith angle nodal points in the look-up tables has increased from 5 [0, 20, 40, 60, 80] to 7 [0, 20, 40, 60, **66, 72**, 80] for all aerosol models. The number of AOD nodal points has changed from 6 [0.0, 0.1, 0.5, 1.0, 2.5, 4.0] to 7 [0.0, 0.1, 0.5, 1.0, 2.5, 4.0, **6.0**] for all aerosol models.

Other changes

- The low limit AI threshold for aerosol retrievals has been lowered to 0.8 over the oceans.

-A field containing the reporting wavelengths [354, 388, 500 nm] has been added to the level2 file and removed from the swath attributes field.

-Information of aerosol layer heights (0.0, 1.5, 3.0, 6.0, 10.0 km) is available in the swath attributes field.

- Row anomaly exclusion rules have been updated

The updated information of row anomaly from the XtrackQualityFlags field in OMI L1b swath file is used for screening row anomaly affected scenes before retrieving aerosol products.

The XtrackQualityFlags field has been added to the Geolocation Fields of level 2 file. The information of bit values for this field is available at the site (http://www.knmi.nl/omi/research/product/rowanomaly-background.php).

Row anomaly screened scenes are also reported as the value of 8 in the AlgorithmFlags field. It is possible to find additional row anomalies not fully characterized in the data so that care must be taken in using data since 2009. A further improved flagging scheme is under development and will be updated periodically as new anomaly develops.

Algorithm version 1.4.2 (March 8, 2012)

Changed scheme to exclude row-anomaly-affected retrievals. No readme file was produced for this version.